Development of Image Sonar Simulator for Underwater Object Recognition

Jeong-Hwe Gu, Han-Gil Joe[1] and Son-Cheol Yu
Department of Creative IT engineering, POSTECH
[1]Ocean Science and Technology Institute, POSTECH
Pohang, Korea
bygu111@postech.ac.kr

***Abstract*—In this paper, two preliminary basic studies of underwater recognition are reported: modeling an image sonar and developing its simulator. The display mechanism of the image sonar is analyzed, and an image sonar model is proposed. The image sonar emits ultrasound beams in the forward direction and then detects those that strike objects and are reflected from their surfaces. The ultrasound beams are modeled as a set of rays, and the image sonar is modeled as an object emitting the rays at a certain position and orientation. The surface of the objects to be observed is modeled as consisting of many small polygons so that any arbitrary shape can be represented by these polygons. Collisions between the ultrasound beams and objects are described in terms of the points at which the rays intersect the polygons. On the basis of the model, a simulator for the image sonar is developed. The sonar images made by the simulator are compared with real sonar images to confirm the validity of the model.**

Keywords—image sonar; modeling; recognition; simulation;

I. INTRODUCTION

Automatic underwater object recognition has great potential for tasks such as object finding, environmental monitoring, and underwater structure installation and maintenance. For example, it can be applied to underwater mine hunting using autonomous underwater vehicles. Underwater optical vision provides the highest-resolution underwater images for recognition, but their visibility is restricted (<2 m), especially in shallow water. Image sonars have become good alternatives for object recognition. In contrast to optical vision, image sonars have high reliability in most underwater environments. Image-sonar-based recognition, however, has many difficulties to overcome for practical use. Owing to the acoustic nature of the underwater environment, sonar images have low resolution and are gray-scale images; that is, the information available for recognition is more limited than in optical images. In addition, the display mechanism of an image sonar is completely different from that of optical cameras. Thus, optical-camera-based models such as the pinhole cannot be applied to sonar image recognition. However, the display mechanism of the image sonar is well understood (Yu, 2012).

First, we briefly describe the display mechanism of the image sonar. Then, the image sonar model is discussed. Next, simulations based on the model are presented. Finally, we present experimental results comparing sonar images from the real sensor and the simulator.

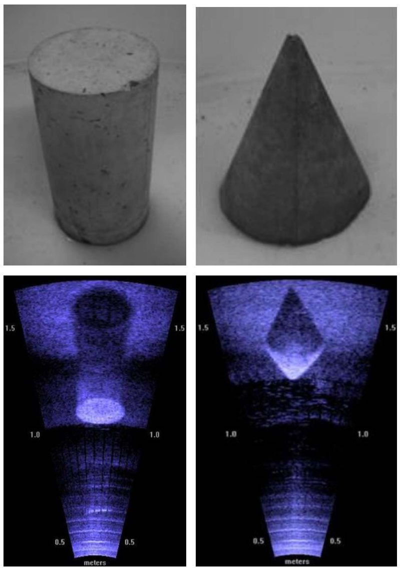

Fig. 1. Sonar images of concrete cylinder and cone

II. DISPLAY MECHANISM OF IMAGE SONAR

The image sonar differs from the optical camera in that it uses ultrasound to form images. It projects ultrasound beams in the forward direction and detects those that are reflected from the surfaces of objects. Fig. 1 illustrates the differences between sonar images and optical images. Both types of images were taken from the same angle and altitude. We used a DIDSON instrument (1.1/1.8 MHz) as the image sonar for this paper.

The basic principle of the image sonar can be explained as follows. If ultrasound beams emitted from the image sonar meet any objects, they are reflected from the surface by backscattering. The image sonar can detect the reflected ultrasound beams with a certain intensity. Because the velocity of the beam underwater and the time interval between sending and receiving the signal are known, it is possible to compute the distance the ultrasound has traveled. Finally, the image sonar can measure how far away the object is. This is how a

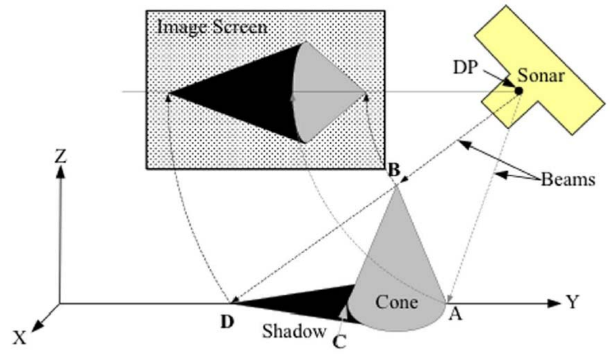

Fig. 2. Display mechanism of image sonar

ship uses ultrasound to measure the depth of the sea floor. The image sonar takes advantage of this phenomenon.

Fig. 2 illustrates how the image sonar can make sonar images using this simple principle. Point DP represents the source and sink of the ultrasound beams. The image screen or sonar image is shown and rotated by 90° for illustration purposes. Point B is the closest point at which the beams can ever meet, so B is mapped onto the lowest point in the sonar image. The lower part of the sonar image is closer to the sensor than the upper part. The beams encounter point A, which is the bottom of the cone, at a greater distance than that for point B, so it lies above point B in the image. The front surface (area from A to B) of the cone blocks the beams from proceeding and meeting objects until point D. This uncovered area is shown in the image as a shadow. The shadow is the area that has no returned beam data and is shown as black in the image. Although this description explains the display mechanism of the image sonar only roughly, it covers the core principle.

The method of constructing sonar images is not reversible mapping. Thus, information is lost during mapping. This is a very important feature of the image sonar. For example, in Fig 2, what if there are other points that are as distant from the sensor as point A? Those could be different parts of the cone or some area of the floor. In this situation, the beam data overlap to the same mapping point. In this case, the one with the brightest intensity wins, and the remaining ones are abandoned. As a result, the single brightest beam data among the other candidates can be seen in the sonar image, which results in loss of information in the image sonar.

There is another important feature of the image sonar. Sonar images are greatly affected by objects' materials. More concretely, they represent objects' surfaces. If the surface of objects is rough, the backscattering of ultrasound beams on the surface is strong, and as a result, the intensity of the returned beams is also high. The strong intensity of the returned beams increases the brightness of sonar images. On the other hand, objects that have smooth surfaces such as metals have dark, blurry edges in the image.

III. Image sonar Model

Sonar images are usually sensitive to changes in viewpoint; that is, a small change in viewpoint can cause a large difference in sonar images. In optical cameras, the display mechanism is associated with the pinhole model. Therefore, changes in the image as the viewpoint changes are predicted using the model.

Our ultimate goal is to recognize objects underwater, so the model we propose should be useful for that purpose. Two types of features are available in sonar images: an object's highlighted areas and shadow areas. Therefore, the model should exhibit the capacity to observe these two features.

In this section, the working mechanism of the image sonar will be modeled through a geometrical description. The model can be divided into two parts: objects and the image sonar. First, they will be dealt with separately, and then we will discuss how to relate the two.

A. *Object*

Objects are modeled according to the following idea. Because ultrasound beams are reflected from the surfaces of objects, we should know the shape of the objects. Normally, the shape or surface of objects is too complex to be represented by analytical equations. However, we can definitely deal with simple plane equations. Therefore, if an object can be described by many small plane patches, we can model its surface. These patches are called polygons. Fig. 3 shows an object whose surface consists of several triangular polygons. This is an example of a curved surface being approximated by polygons. If more polygons are used, the surface is smoother. The simplest polygon is the triangle because three points define a plane. These three points are defined in the global coordinate system. We will introduce the local coordinate system in the following section. If we consider the points as the position vectors, the normal vector N of a polygon is expressed as follows (refer to Fig. 3).

$$\overrightarrow{N} = (\overrightarrow{p_2} - \overrightarrow{p_1}) \times (\overrightarrow{p_3} - \overrightarrow{p_1}) \tag{1}$$

The equation of the plane satisfies the following condition.

$$\overrightarrow{N} \cdot (\overrightarrow{p} - \overrightarrow{p_1}) = 0 \tag{2}$$

Point p is an arbitrary point on the plane. In this way, objects can be modeled.

B. *Image sonar*

The image sonar is a sensor that can be attached to a ship or underwater vehicle, so it can move by either translation or rotation. This fact requires us to introduce another coordinate system to describe the ultrasound beams. Therefore, we need two coordinate systems: global coordinates and local coordinates. As stated above, the equation of objects is given in the global coordinate system, whereas the equation of the ultrasound beams is given in the local coordinate system. A coordinate transformation that can be represented in terms of Euler's angles and the translation vector links the two coordinate systems. However, we will omit the detailed process and only use the concept.

The upper panel of Fig. 4 shows how the image sonar projects ultrasound beams. The ultrasound beam is a vertical plane that proceeds in a fan shape. This plane sweeps rapidly

$$\vec{p} = t\vec{v} \;\; ; \;\; (t \geq 0) \tag{3}$$

or

$$\begin{bmatrix} p_x \\ p_y \\ p_z \end{bmatrix} = t \begin{bmatrix} \cos\phi\cos\theta \\ \cos\phi\sin\theta \\ \sin\phi \end{bmatrix} \tag{4}$$

where point p is an arbitrary point on the line, and $\vec{v}$ is the normalized direction vector. The origin of the coordinate system is considered to be the source of the beams.

The last step is to relate the two equations. The reflection of the ultrasound beam from objects can be modeled as an intersection of the planes and lines. Here the planes represent objects, and the lines represent beams. If a line meets a plane, the distance from the source (origin) to the crossing point can be computed, and this distance will be used to draw the sonar images, which is the same as in the real image sonar.

The distance value can be found by the following procedure. We will assume that a line passes through a polygon. First, we should match the coordinate systems. Let $T(\cdot)$ be the coordinate transformation function that converts coordinates from the global to the local system. Then the three points of the polygon and the normal vector are transformed as

$$\begin{aligned} \overrightarrow{p_1}' &= \mathrm{T}(\overrightarrow{p_1}) \\ \overrightarrow{p_2}' &= \mathrm{T}(\overrightarrow{p_2}) \\ \overrightarrow{p_3}' &= \mathrm{T}(\overrightarrow{p_3}) \\ \overrightarrow{N}' &= \mathrm{T}(\overrightarrow{N}) \end{aligned} \tag{5}$$

We obtain two equations for the line and plane.

$$\overrightarrow{N}' \cdot (\vec{p} - \overrightarrow{p_1}) = 0 \tag{6}$$

$$\vec{p} = t\vec{v} \tag{7}$$

where point p is the crossing point. If we solve the equations for t,

$$t = \frac{\overrightarrow{N'} \cdot \overrightarrow{p_1}}{\overrightarrow{N'} \cdot \vec{v}} \tag{8}$$

If we substitute this into (8), we obtain

$$\vec{p} = \frac{\overrightarrow{N'} \cdot \overrightarrow{p_1}}{\overrightarrow{N'} \cdot \vec{v}} \vec{v} \qquad ; (\overrightarrow{N'} \cdot \vec{v} < 0) \tag{9}$$

where condition $\overrightarrow{N'} \cdot \vec{v} < 0$ is needed to ensure that the beam meets the outer surface of the polygon.

The important point is that the crossing point should be inside the polygon. To check this, we should use the crossing point to construct three vectors that have same direction as the normal vector, as shown in Fig. 5. For these three vectors, the following three equations should be satisfied for the crossing point to be inside the polygon.

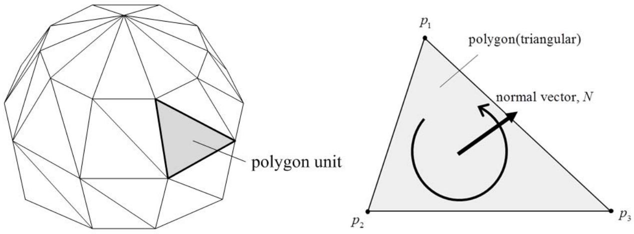

Fig. 3. Object approximated by ploygons and unit polygon(triangle)

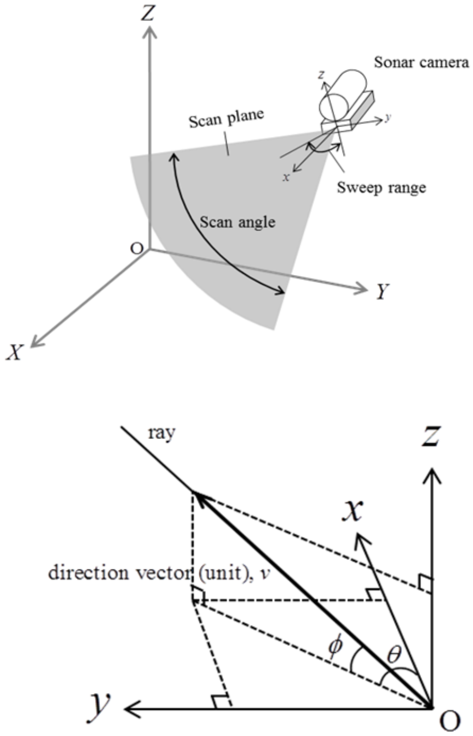

Fig. 4. Ultrasound beam of image sonar in the form of a vertical plane (top) , model of ultrasound beam as a line (bottom)

from side to side to detect objects. In this way, the image sonar can cover a certain area range in the forward direction.

In the model, the ultrasound beams are considered as a set of lines, in accordance with the idea that many lines can approximate a plane. The lower panel of Fig. 4 shows one of those lines. Each line has its own ϕ and θ that define its direction. The angles ϕ and θ range from -15 to 15°. There are 1000 lines in direction ϕ to approximate the scan plane and 96 in direction θ to approximate the sweeping motion. Attenuation and diffusion of ultrasound beams are ignored in the model.

The line equation is stated as follows in the local coordinate system,

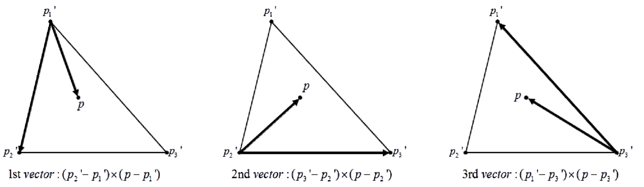

Fig. 5. Three vectors having the same direction as the normal vector

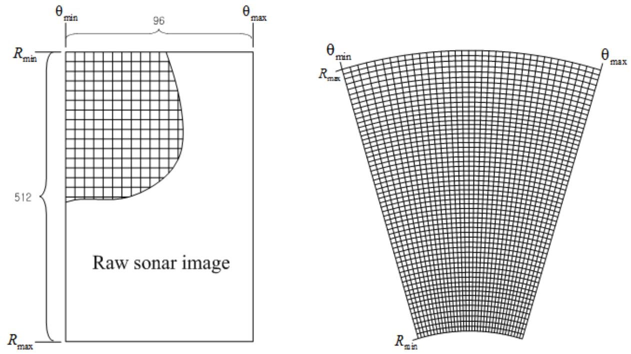

Fig. 6. Raw form of sonar image (left) and sector form of sonar image(right)

$$((\overrightarrow{p_2}' - \overrightarrow{p_1}') \times (\vec{p} - \overrightarrow{p_1}')) \cdot \overrightarrow{N}' \geq 0$$
$$((\overrightarrow{p_3}' - \overrightarrow{p_2}') \times (\vec{p} - \overrightarrow{p_2}')) \cdot \overrightarrow{N}' \geq 0 \quad (10)$$
$$((\overrightarrow{p_1}' - \overrightarrow{p_3}') \times (\vec{p} - \overrightarrow{p_3}')) \cdot \overrightarrow{N}' \geq 0$$

Finally, the absolute distance value, which gives the distance to the crossing point, needs to be computed. If we compute the absolute value of (9),

$$|p| = \left| \frac{N' \cdot p_1'}{N' \cdot v} v \right| = \left| \frac{N' \cdot p_1'}{N' \cdot v} \right| |v| = \left| \frac{N' \cdot p_1'}{N' \cdot v} \right| \quad \because |v| = 1 \quad (11)$$

In this way, every line is checked to determine if it meets a polygon. After all the checking, each line has three quantities: ϕ, θ, and $|p|$.

These three quantities are used to draw the sonar image. Fig. 6 (left) shows the raw version of the sonar images. Angle θ corresponds to the x axis, and $|p|$ corresponds to the y axis in the image. Thus, θ and $|p|$ determine the position in the image. The intensity value at a specific position is determined by what the lines meet. For example, if a line meets an object, the intensity value will be 1, which is white. If the line meets the floor, the value will be 0.5, which is gray. The angle ϕ is used to select the higher-intensity values of the lines. That is, if two lines have the same θ and $|p|$ but different ϕ, the one with the higher intensity value is selected to occupy the position. This follows from the assumption that lines with same θ are in the same scan plane. After the raw image is drawn, it is transformed into the sector form (Fig.6, right) which is easier for human eyes to recognize.

IV. Simulation

We made a program that simulates the image sonar by applying the model. A cube-shaped object is used in the simulation because it is easy to make by hand. Fig. 7 shows a conceptual image of the cube being used. A cube has 8 vertices and 12 polygons. The vertices are numbered in order to compute the normal vectors of each polygon. The reflection of the cube will be drawn in white, whereas that of the floor or ground on which the cube lies will be drawn in gray.

The program executes the algorithm shown in Fig. 8. The order is the same as that described in the previous section. In addition, we took advantage of the OpenCV library to handle the image files.

V. Experiment

We performed an experiment to verify the model of the image sonar. To conform to the object shape in the simulation, we made a cube having a length of about 0.2 m from concrete. Concrete was chosen as the material because the image sonar can view it with high intensity owing to the strong backscattering on the surface. Fig. 9 shows the cube used in the experiment and the experimental environment. We obtained sonar images of the cube in the experiment. The underlying wooden board helps the image sonar to observe the shadow of the object clearly. In this experiment, the observing angle of the image sonar is classfied into three types: high, mid, and low angle. This is because it is hard to measure the image sonar's observing angle.

Figs. 10 and 11 compare the experimental and simulated sonar images. Note that the figures have different viewing directions. The first rows of each figure show optical images of the object that correpond to the sonar images below.

The images exhibit certain characteristics or differences. First, the real sonar images have considerable noise, whereas the simulated images have none. Second, the simulated images have many spots in the upper part, especially at low observing angles. This is due to the gaps between the lines that represent the ultrasound beams. The gaps become larger as the lines proceed, and the result is seen in the images. Third, in Fig. 11, there is an intensity difference between the top face and side face of the cube. At high angles, the top face has a higher intensity than the side faces, whereas at low angles, the side faces have higher intensity. This is due to the angle of reflection at which the ultrasound beams meet the surface. However, the simulated images have the same intensity regardless of the face.

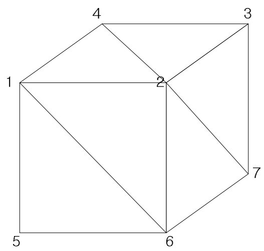

Fig.7. Conceptual image of cube used in the simulation

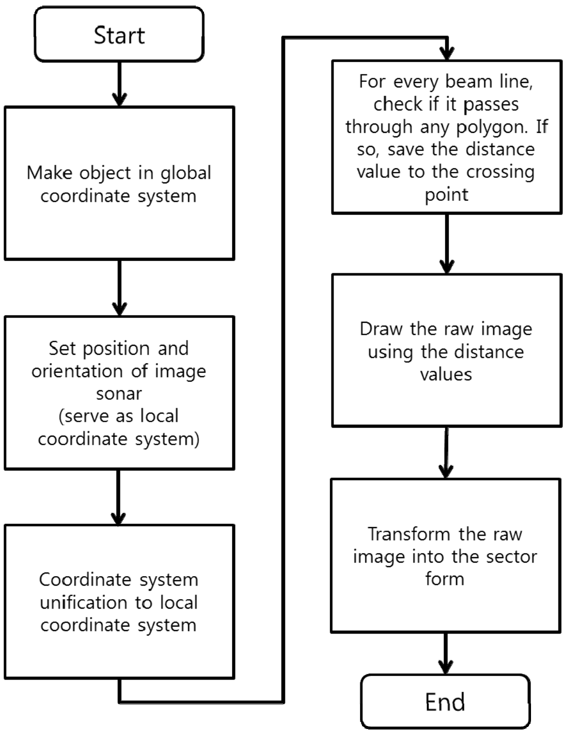

Fig. 8. Flow chart of the simulator

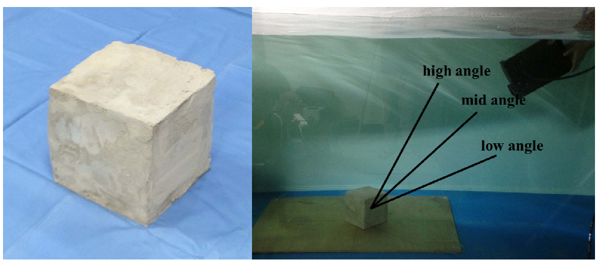

Fig. 9. Picture of the cube (left) and the experimental environment (right)

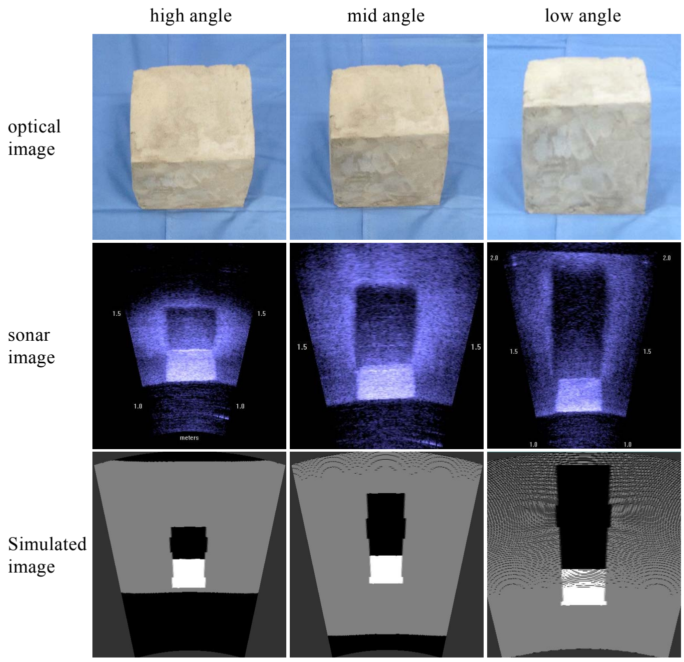

Fig. 10. Comparison of experimental and simulated sonar images of cube when two sides are optically visible

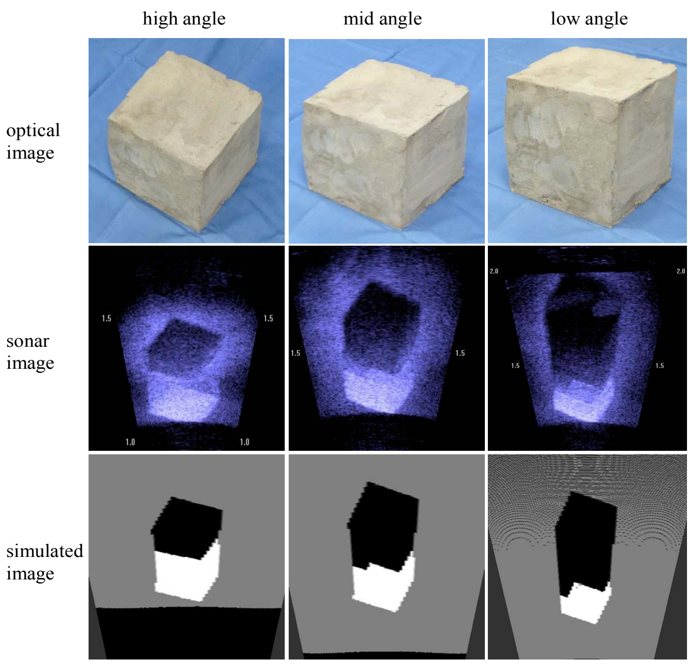

Fig. 11. Comparison of experimental and simulated sonar images of cube when three sides are optically visible

Despite these differences, the overall shapes are very similar. This similarity confirms the validity of the model; thus, it is acceptable to model the ultrasound beams as lines.

VI. Conclusion

In this paper, we introduced the display mechanism of the image sonar and proposed an image sonar model. The core concept of the model is the use of polygons for object representation and geometrical lines for the ultrasound beams. On the basis of the model, an image sonar simulator was developed. We verified the model by an experiment in which real sonar images were compared to the simulated images. A qualitative comparison shows good agreement in the shape of the object and its shadow.

However, we have an important problem to overcome regarding the construction of arbitrary objects from polygons. To generate a complex object, some existing program that can work with a graphic library should be used along with the simulator. This remains an unsolved problem. For the next study, underwater recognition will be examined using the image sonar model and the simulator.

ACKNOWLEDGMENT

This research was supported by the MSIP IT Consilience Creative Program(NIPA-2013-H0203-13-1001), Korea and a part of the project titled "Long-term change of structure and function in marine ecosystems of Korea" and Gyeongbuk Seagrant Program funded by the Ministry of Oceans and Fisheries, Korea.

REFERENCES

[1] S.C. Yu, Z. Teng, and D.J. Kang, "Modeling of High-Resolution 3D sonar for Image Recognition", Intl. J. of Offshore and Polar Engineering, vol. 22, No. 3, pp. 186-192, 2012

[2] L. Eric, "Mathematics for 3D game programming and computer graphics", 3rd Ed, Course Technology, 2011

[3] S.C. Yu, "Development of Real-Time Acoustic Image Recognition System Use by Autonomous Marine Vehicle", J Ocean Eng., Elsevier, Vol. 35, Issue 1, pp.95-105, 2008

[4] Etter, P.C.,"Underwater Acoustic Modeling and Simulation: Principles, Techniques and Applications, Spon Press, 2003

[5] DIDSON Website, www.DIDSON.com

[6] Burdic, "Underwater Acoustic System Analysis", Prentice-Hall Press, 1984

[7] Urick, "Principles of Underwater sound", 3rd Ed, McGraw-Hill Book Company, 1983

[8] Lurton, "An Introduction to Underwater Acoustics", Praxis Publishing press, 2002

[9] Foresti, Murino V. and Regazzoni, "A voting-Based Approach for Fast Object Recognition in Underwater Acoustic Images", J Oceanic Eng., IEEE, Vol. 22, No. 1, pp57-65, 1997

[10] S.C. Yu, T.W. Kim, G. Marani, and S.K. Choi, "High Resolution Acoustic Camera Model-Based Object Recognition for AUVs", Proc. 15th Int. Conf. on Unmanned Untethered Submergible Tech., 2007